Electronic Supplementary Material (ESI) for Nanoscale.

Supplementary materials for

Cell mechanics demonstrates resistance to malignant transformation in naked mole rat fibroblasts

Nadezda Makarova[1], Vivekanand Kalaparthi[1†], Andrei Seluanov[2], Vera Gorbunova[2], Maxim Dokukin[1,3,4], Igor Sokolov[1,6,7,]*

[1]Department of Mechanical Engineering, Tufts University, Medford, MA 02155, USA

[3]NanoScience Solutions, Inc., Arlington, VA 22203, USA

[4]Sarov Physics and Technology Institute, MEPhI, Sarov, Russian Federation

[6]Department of Biomedical Engineering, Tufts University, Medford, MA 02155, USA

[7]Department of Physics, Tufts University, Medford, MA 02155, USA

* Email: Igor.Sokolov@Tufts.edu

1. Examples of force curves collected with AFM (raw data is shown)

The examples are shown in Fig.S1. An abnormal behaiours of the curve at large Z is a combination of the nanoscope software bug and non-linearity of the photodetector of the AFM scanner. Those parts of the curve are not considered for the analysis and shown here for information only.

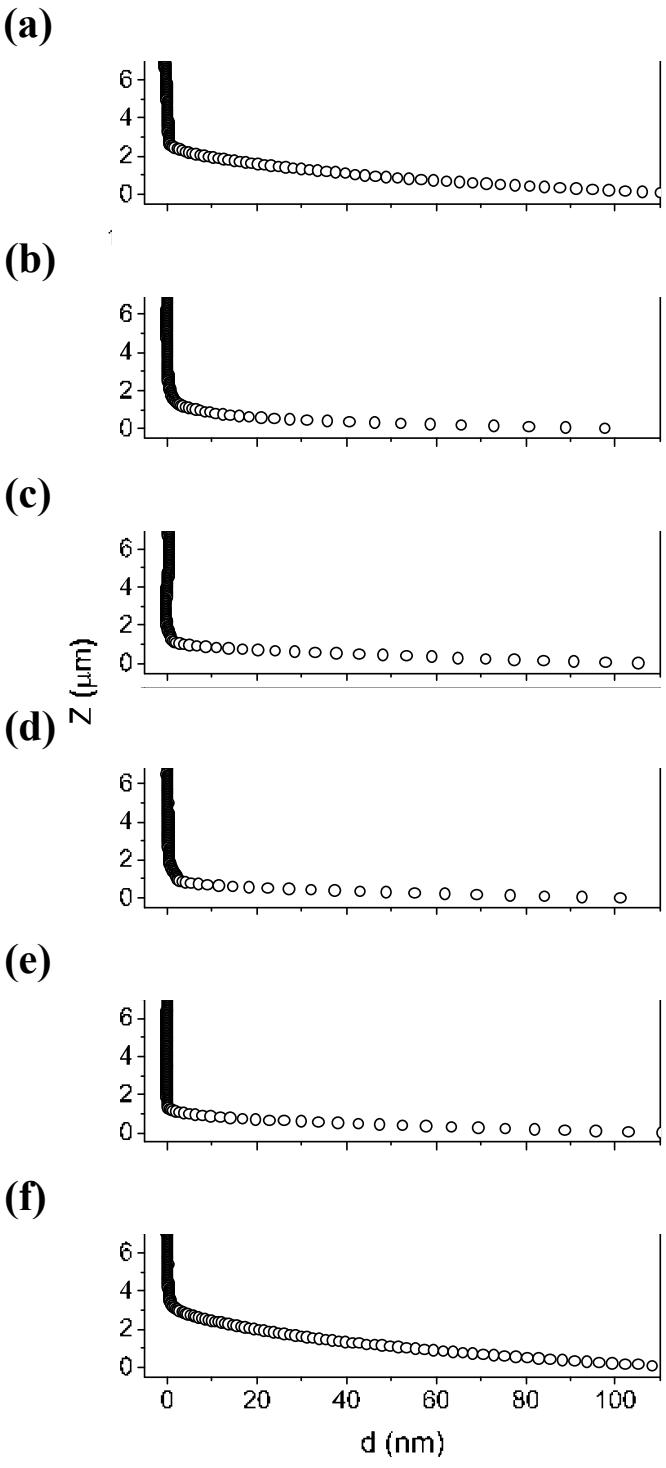

Fig.S1. Example panel of 6 raw AFM indentation force curves that were processed by the brush model. (a – c) shows NMR force curves. (d – f) shows mouse force curves. The used for the analysis approach parts of the curves are shown.

2. An example of data processing

Reperesentative examples processing the force curves (raw data) thought the brush model are shown for the cases of single and double brishes in Figs S2 and S3, respectively.

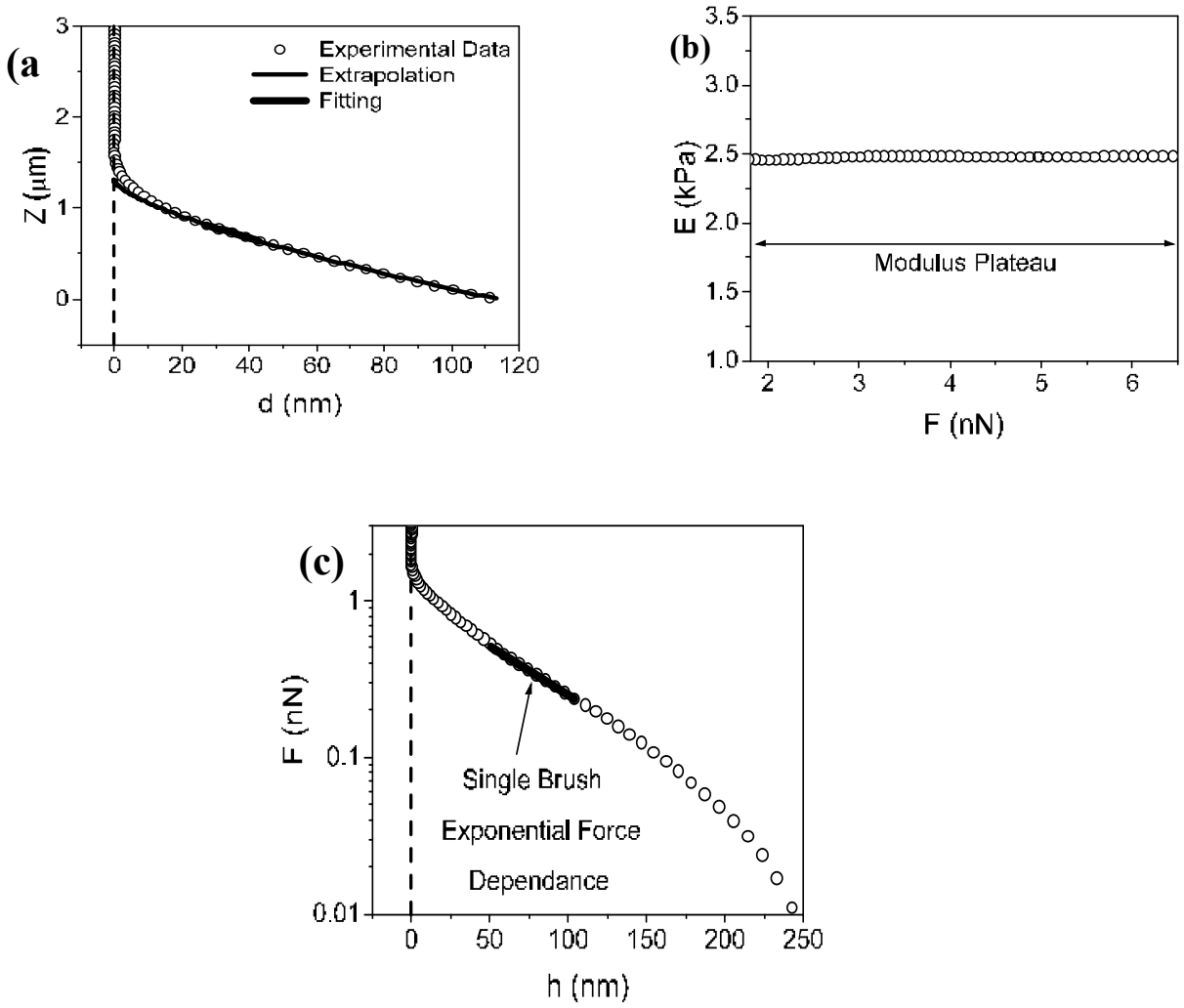

Fig.S2. An example shown is an NMR control cell with a single brush behavior.
(a) row data, the dependence of the deflection of the cantilever *d* on the vertical position of the sample *Z*. (b) the dependence of the effective Young's modulus on the load force. The modulus corresponding to the plateau is treated as the modulus of the cell body. The specific example gives the valley of the modulus E = 2.1 kPa. Note: this dependence is for the case of fixed Z_0.
(c) The force due to brush. This is an example of single brush with the fitted brush parameters *L* = 450 nm, and *N* = 200 $1/\mu m^2$.

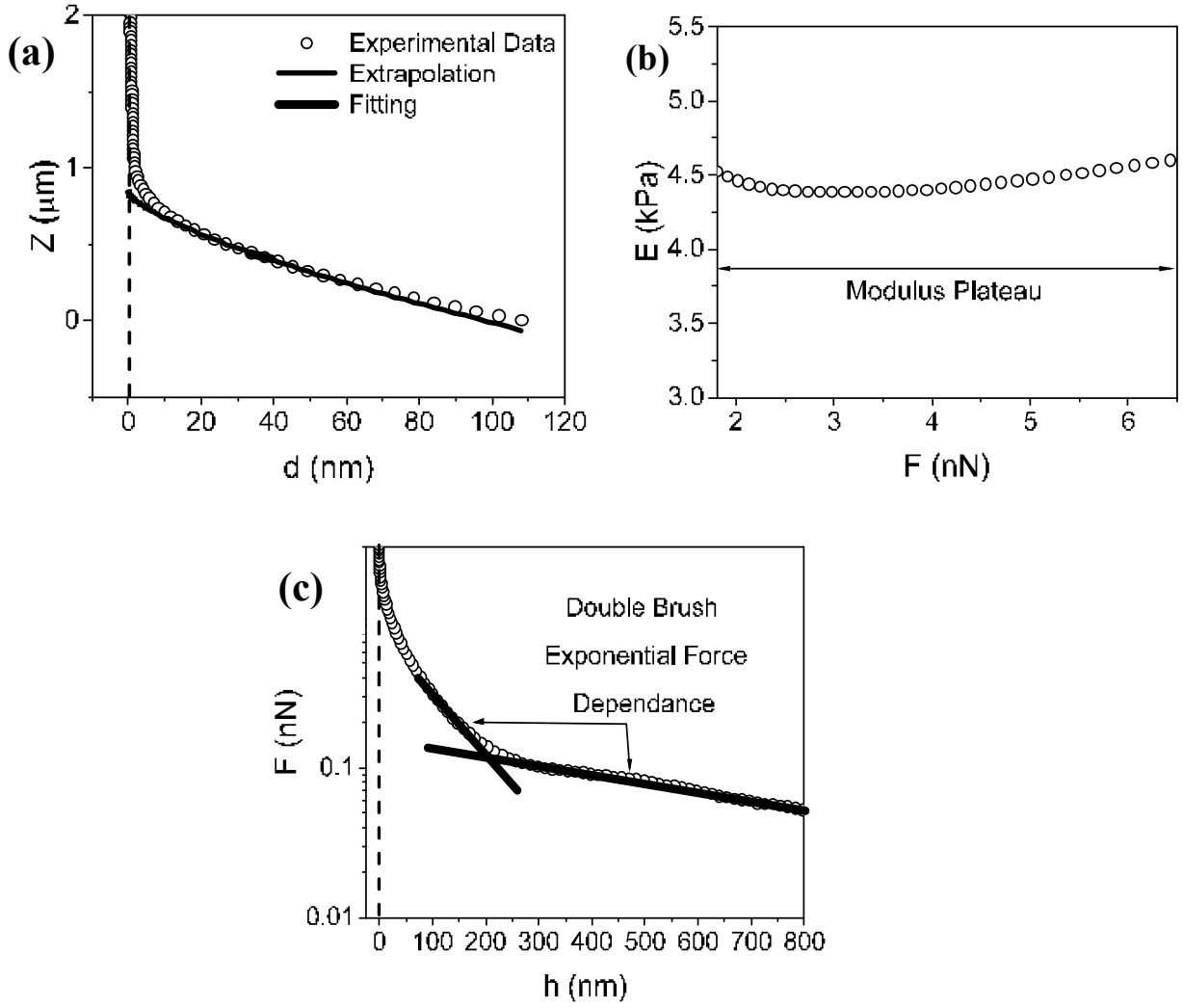

Fig.S3. An example shown is an NMR cell with a double brush behavior.

(a) row data, the dependence of the deflection of the cantilever *d* on the vertical position of the sample *Z*.

(b) the dependence of the effective Young's modulus on the load force. The modulus corresponding to the plateau is treated as the modulus of the cell body. The specific example gives the valley of the modulus E = 3.6 kPa. Note: this dependence is for the case of fixed Z_0.

(c) The force due to brush. This is an example of single brush with the fitted double brush parameters L_1 = 280 nm and N_1 = 390 $1/\mu m^2$, and L_2 = 6500 nm and N_2 = 8 $1/\mu m^2$.

3. Holding the baseline of the force curves during vertical ramping

Since the approach speed is nonzero, it is natural to expect possible hydrodynamic/viscous resistance when the AFM probe approaches the cell surface. To exclude such effect, the approach speed was chosen to be a relatively small (27 μm/sec), but not too small to avoid cell migration the measurements. To verify that this speed does not bring us a substantial hydrodynamic resistance, we recorded the force curves over the area of petri dish which is free of cells. It has to be noted that some parts of petri dish could be coded with the organic debris of the culture medium. That is why, one has to try different force curves to see the sharpest deflection of the AFM cantilever, which corresponds to the cleanest part of the petri dish. Figure S4 shows an example of such a force curve. The baseline was hold at zero within 0.22 nm or 13pN (RMS) when the AFM tip is approaching the Petri dish surface from 7 to 1 μm. If we apply the brush model to calculate a possible brush near the contact, it gives us L = 1.4 μm, and N = 10 1/μm^2. It makes sense to combine these parameters to the size of the brush, $L*N$ as defined in the main text and also in other previous publications. One see that the size of this "brush" is very small compared to even the weakest cell brushes (14 μm^{-1} versus 100-1000 μm^{-1} , see Figure 6). Thus, one can conclude that the effect of hydrodynamic/viscous resistance can be neglected.

It is useful to note that this procedure can definitely be done on a clean glass slide or a clean petri dish. However, the use of the same dish which has the sample cells has a lot of advantages. First, these force curves are naturally collected with the force volume images, in which the empty parts of petri dish are also scanned. Secondly, verifying the presence of these "empty" force curves allows to check a) the lack of possible contamination of the AFM probe, and b) the stability of the calibrated sensitivity of the photodetector.

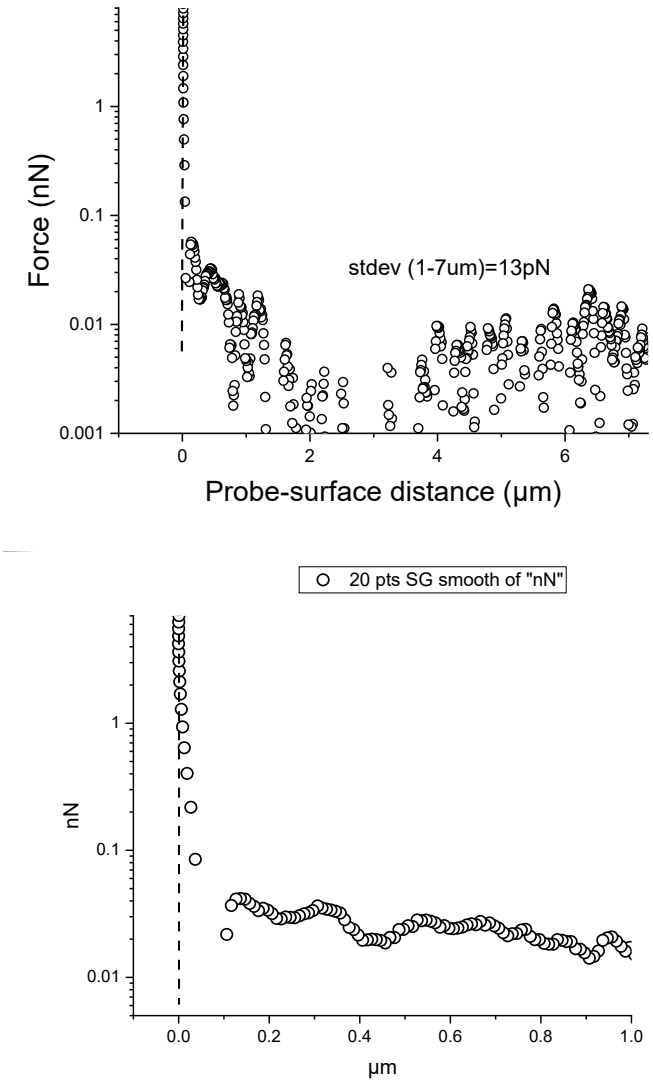

Fig.S4. An example of the force curve of the AFM cantilever approaching and touching the surface of a Petri dish away from cells. Two different vertical ranges are shown: (top) 0-7 μm, (bottom) 0-1 μm.

4. Bottom Substrate Effects

It is important not to overestimate the Young's modulus of the cell body by ignoring a possible rigid substrate, the culture dish on which the cells are sitting. The effect was described in the literature [1]. The following correction should be used for the Hertz model:

$$h = Z - Z_0 + d + \left(\frac{9}{16}\frac{kR^*d}{E}\right)^{\frac{2}{3}}\left(\frac{1}{1+1.133x+1.283x^2+0.769x^3+0.0975x^4}\right)^{\frac{2}{3}} \quad (1)$$

where Z represents the relative vertical scanner position of the cantilever, d is the cantilever deflection, Z_0 is the undeformed position of the cell body, h is the separation between the cell body and AFM probe, E is the elastic modulus of the cell body, k is the cantilever spring constant, and

$$x = \frac{1}{ht}\sqrt{\frac{Z_0-d-Z}{R^*}} \quad (2)$$

where ht is the cell height. The effective radius, R^*, is defined as:

$$R^* = \sqrt{\frac{R_{probe}+R_{cell}}{R_{probe}R_{cell}}} \quad (3)$$

where R_{probe} and R_{cell} are the radii of curvature of the AFM probe and cell, respectively.

For the cell example in Fig. S2, indentation into the cell at the determined modulus plateau is 0.65μm, and the cell is 13.5 μm in height. Indentation is 5% of the cell height. Correcting for the glass substrate, modulus decreases to 2.2 kPa from 2.5 kPa, or by 12%. Similar results can be obtained for the force curves shown in Fig. S3. The maximum indentation depth at the determined modulus plateau is 0.42 um, and the cell height is 8.2 μm. By correcting for the substrate, the Young's modulus decreases to 3.9 kPa from the 4.4 kPa, which is about the 11%. These examples are quite representative. So we can say that the error due to ignoring the bottom effect is of the order of 10-12% in this work. This is comparable or smaller than the uncertainty that may come from the measurements of the spring constant of the AFM cantilever (5-20%) [2-4]. Therefore, we neglect this correction in the present work.

5. Defining the cell geometry

The cell geometry, the cell height and radius were defined from the the force volume images as described in ref. [5]. Fig.S5 show the example of processing of the force-volume hight image of the cell (corrected by the deformation of the cell body) and calculation of the cell radius.

The average height of NMR cells was 8.5 μm and 6 μm for mouse cells. Indentation depth (of the cell body) used to calculate the Young's modulus were ~0.5 microns. Therefore, the bottom effect was negligible. The curvature radius of the top part of the cells was at a range of 9.0 – 160 μm (NMR) and 6.0 – 170 μm (mouse).

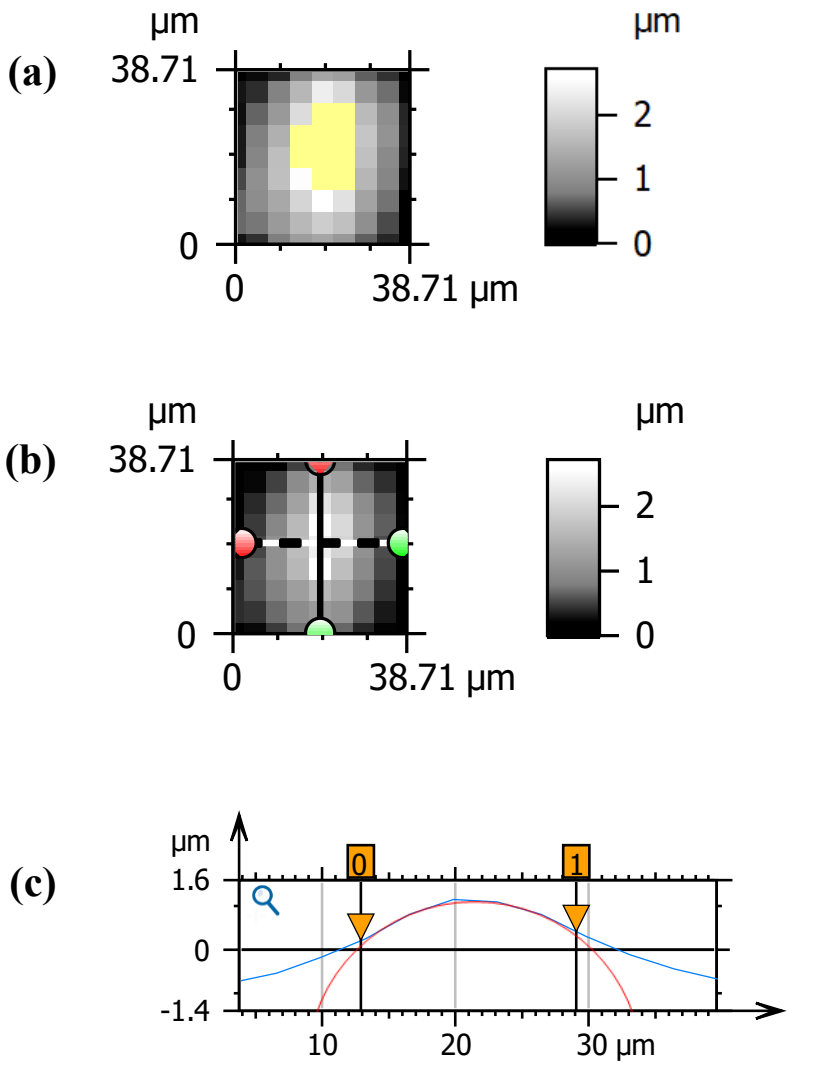

Parameters	0-1	Unit
Radius	37.51	µm

Fig.S5. representative (a) height image of a NMR skin fibroblast cell used to find the cell radius. Area in the center (on top) of the cell where force curves were extracted is highlighted by yellow color, (b) the two chosen cross section to find the radius of curvature, (c) radius of the cell calculated from the horizontal cross section. The radius used for the final calculation was derived as a geometrical average from radii taken from the vertical and horizontal cross sections.

Supplementrary References

1. E. K. Dimitriadis, F. Horkay, J. Maresca, B. Kachar and R. S. Chadwick, *Biophys J*, 2002, **82**, 2798-2810.
2. P. H. Wu, D. R. B. Aroush, A. Asnacios, W. C. Chen, M. E. Dokukin, B. L. Doss, P. Durand-Smet, A. Ekpenyong, J. Guck, N. V. Guz, P. A. Janmey, J. S. H. Lee, N. M. Moore, A. Ott, Y. C. Poh, R. Ros, M. Sander, I. Sokolov, J. R. Staunton, N. Wang, G. Whyte and D. Wirtz, *Nature Methods*, 2018, **15**, 491-498.
3. N. Guz, M. Dokukin, V. Kalaparthi and I. Sokolov, *Biophysical Journal*, 2014, **107**, 564-575.
4. Z. C. Ying, M. G. Reitsma and R. S. Gates, *Review of Scientific Instruments*, 2007, **78**.
5. M. Dokukin, Y. Ablaeva, V. Kalaparthi, A. Seluanov, V. Gorbunova and I. Sokolov, *Biophysical Journal*, 2016, **111**, 236-246.